Pharm Res (2014) 31:3019–3030
DOI 10.1007/s11095-014-1395-2

RESEARCH PAPER

Self-assembled Chitosan-Ceramide Nanoparticle for Enhanced Oral Delivery of Paclitaxel

Gantumur Battogtokh • Young Tag Ko

Received: 16 January 2014 / Accepted: 15 April 2014 / Published online: 14 May 2014

ABSTRACT

Puspose We aimed to synthesize novel ceramide-chitosan (CS-CE) conjugate that forms stable polymeric nanoparticle capable of functioning as efficient carriers of hydrophobic drug such as Paclitaxel (PTX) for oral delivery.

Methods Chitosan (3–5 kDa) was conjugated with ceramide by using a DSC coupling reagent to improve its hydrophobic drug entrapment capacity. The structure of the conjugate was determined by proton (^{1}H) NMR and FT-IR spectrometry. Size distribution and zeta potential were measured by DLS and PTX content in the cells and plasma was determined by HPLC and LC-MS.

Results Under suitable conditions, the CS-CE self assembled to form colloidally stable nanoparticles with a mean diameter of ~300 nm. Further, PTX was incorporated into the CS-CE nanoparticle with 96.9% loading efficiency and 12.1% loading capacity via an emulsion-solvent evaporation method. The PTX-loaded CS-CE (PTX-CS-CE) showed sustained release of PTX and a comparable cytotoxic efficacy to that of free PTX on B16F10 melanoma and MCF-7 human breast adenocarcinoma cell lines. The empty nanoparticles showed no toxicity, indicating that the copolymer is safe to use in drug delivery. In addition, higher cellular uptake and slightly better pharmacokinetic parameters were obtained for PTX-CS-CE nanoparticle compared to free PTX.

Conclusion The polymeric nanoparticle of CS-CE represents a promising nanocarrier of hydrophobic drug for oral delivery.

KEY WORDS ceramide · chitosan · paclitaxel · polymeric nanoparticle · self assembling

G. Battogtokh • Y. T. Ko (✉)
College of Pharmacy, Gachon University, 191 Hambakmoe-ro Yeonsu-gu, Incheon 406-799, South Korea
e-mail: youngtakko@gachon.ac.kr

INTRODUCTION

Poor water solubility and adverse side effects of anticancer drugs have limited their therapeutic applications (1, 2). In order to circumvent the problem of solubility, use of nanosized drug carriers such as micelles, liposomes, dendrimers, and polymeric nanoparticles have been extensively studied (1, 3). Although using nanocariers could solve the problem related to solubility of hydrophobic drugs in systemic delivery, development of oral delivery of anticancer drugs is still a challenge because the nanocariers easly dissociate due to acidic condition of gastrointestinal (GI) tract system (4). Oral administration would be highly beneficial for the patients to reduce inconvenience, pain, risks of complications as well as the development of chronic treatment schedules, which would decrease the cost of the therapy (5).

Polymeric nanoparticles self-assembled from copolymers typically consist of an inner hydrophobic core and an outer hydrophilic shell corona. The hydrophobic core efficiently encapsulates poorly water-soluble drug molecules, while the shell protects the drug from aqueous environments and stabilizes the polymer nanoparticles against *in vivo* recognition by the reticuloendothelial system (1, 2, 6).

Among the nanocarriers studied, polymeric nanoparticles prepared from chitosan and its derivatives are highly favored owing to their biocompatibility, biodegradability, and nontoxicity (7, 8). Chitosan possesses mucoadhesive characteristics as well as the ability to reversibly modulate the integrity of epithelial tight junctions, which is an adventage of chitosan to use as a drug carrier for oral delivery (4, 9). Chitosan is a long nonbranched polysaccharide similar to cellulose derivatives in which the hydroxyl group at the C_2 position has been replaced with an amino group (10). The reactive hydroxyl and amino groups in chitosan can be chemically modified to produce tailor-made analogs, for specific applications (8). However, applications of chitosan are limited

because of its poor water solubility (11). Additionally, their soluble salts block the reactivity of amino groups (11).

Thus, hydrophobically modified chitosans (with deoxycholic acid (12), linolenic acid (13), linoleic acid (14), oleic acid (15), salicylic acid (16), etc.) form nanosized self-assembled aggregates, and show promise as carriers for drug delivery. Although longer hydrophobic chains and bulky hydrophobic groups help stabilize the micellar structure and protect the drug molecules from the environment (17), their loading capacity is limited (18). In this regard, self assemblies of chitosans with a hydrophobic block containing two chains could exhibit improved drug loading capacity (19).

Ceramide, a component of cellular membranes composed of two hydrophobic chains, a sphingosine and a fatty acid (20), which is known to be an excellent hydrophobic core of nanoparticle (21), thereby efficiently encapsulating hydrophobic drugs and facilitating sustained drug release (2).

Therefore, we aimed to synthesize a chitosan-ceramide (CS-CE) graft copolymer suitable for the formation of colloidally stable polymeric nanoparticles that can be used as efficient drug carriers (Fig. 1). It was hypothesized that CS-CE will likely form nanoparticles with a mucoadhesive chitosan corona and hydrophobically stabilized CE core in the presence of hydrophobic drugs, providing an attractive oral drug delivery system for water insoluble drugs (4, 22, 23). In this study, the anticancer agent, paclitaxel (PTX) was used as a model drug to prepare PTX-loaded CS-CE nanoparticle.

MATERIALS AND METHODS

Materials

All reagents were purchased from Sigma-Aldrich (St. Louis, Missouri) and Tokyo Chemical Industry (Tokyo, Japan) unless otherwise stated. Chitosan (3–5 kDa) with 75% deacetylation was purchased from Kitto Life (Seoul, South Korea). Ceramide 3B (DS-Y30; N-oleoyl phytosphingosine) was obtained from Doosan Biotech (Yongin, South Korea).

Synthesis of CS-CE Conjugate

For the synthesis of CS-CE conjugate, 50 mg (0.087 mmol) of ceramide in 5 mL of anhydrous tetrahydrofuran (THF) was reacted with 66.1 mg (0.26 mmol) of *N*, *N*-disuccinimidyl carbonate (DSC) in 1 mL of THF in the presence of 31 mg (0.26 mmol) of 4-(dimethylamino) pyridine in 1 mL of THF, for 6 h at room temperature (RT). Progress of the reaction was monitored by thin-layer chromatography (TLC) by using methanol/dichloromethane (DCM) (4:96) and hexane/ethylacetate (50:50) as eluents. After the reaction was completed, the solvent was removed by a rotary evaporator. To the dried residue, 70 mg (0.017 mmol) of chitosan pre-dissolved in 5 mL of dimethylsufoxide (DMSO) (at 5:1 M ratio of CE:CS) at 50°C for 30 min, was added and stirred at 50°C for 48 h. Progress of the reaction was monitored by TLC. To this reaction mixture, 100 mL of THF was added to precipitate the product from the DMSO solution. The precipitate formed was filtered by suction, and the residue was washed with THF several times to remove remaining reagents and impurities. The solids obtained were dried under vacuum and characterized by proton nuclear magnetic resonance (^{1}H NMR) spectroscopy (Brucker, 600 MHz, Billerica, MA) as well as fourier transform infrared (FT-IR) spectroscopy (Brucker, Billerica, MA). The yield of the product obtained was 67.25%. ^{1}H NMR (in DMSO-d_6, 600 MHz) δ (ppm): 7.8 (br s, NH-acetyl of CS), 7.58 (br s, NH of CE), 5.33 and 5.29 (m, CH = CH of CE), 4.7–4.0 (m, −C**H**-OH, C**H**-NH, CH_2-O of CE), 4.28 (m, ^{1}CH-O of CS), 3.9–3.39 (m, 3–, 4–, 5–, 6–, 1′–, 3′–, 4′–, 5′–, 6′-H in $GluNH_2$ and GluNHAc of CS), 3.04 (m, 2-H in $GluNH_2$ of CS), 2.44 (m, 2'-H in GluNHAc of CS), 2.2–1.95 and 1.61–1.41 (m, −C**H$_2$**-C**H**OH and -C**H$_2$**-CONH of CE), 1.79 (br.s, CH_3-O of CS), 1.21 (m, alkyl (−CH_2-) of CE), 0.831 (t, CH_3 of CE). FT-IR (v, cm^{-1}): 3,364.6 (m, N-H str, amide of CS), 2,922.7 (m, C-H str, alkane of CE), 1,654.2 (s, C = O str, amide I band (CO-NH) of CS), 1,556.4 (s, N-H str, amide II band of CS), 1,015.7 (s, C-OH str, primary and secondary alcohol of CS and CE).

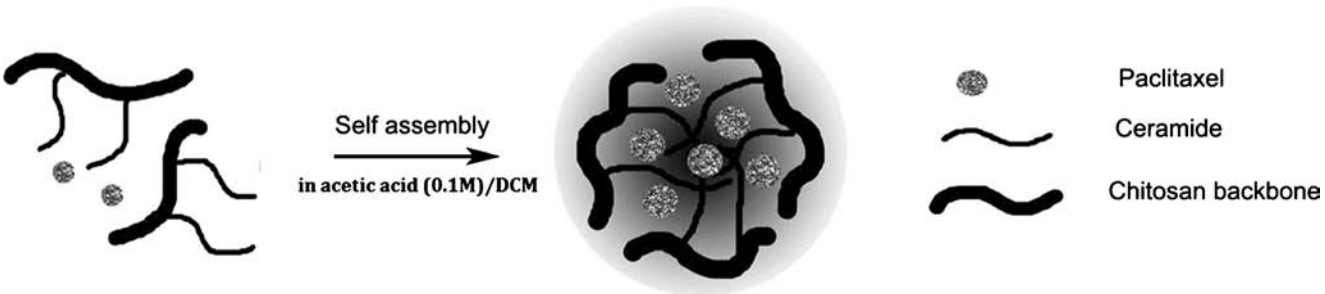

Fig. 1 Schematic diagram showing self-assembly of paclitaxel-loaded polymeric nanoparticles of chitosan-ceramide copolymer (CS-CE).

Preparation of PTX-Loaded CS-CE Nanoparticle

PTX-loaded CS-CE nanoparticle was prepared following a previously reported method with minor modifications (15, 24). Briefly, 21.5 mg of CS-CE was dissolved in 5 mL acetic acid solution (0.1 M) by stirring at RT for 1 h. To the solution, 2.7 mg of PTX in 500 μL DCM in a ratio of 8:1 polymer/drug (*w*/*w*) was added and stirred for 1 h. The resulting emulsion was sonicated for 10 min by using a bath type sonicator (Branson, Danbury, CT). DCM was evaporated at RT with stirring overnight or under reduced pressure for 2 h by rotary evaporator. The solution was homogenized at 3 bar for 10 cycles by high-pressure EmulsiFlex-B15 homogenizer (Avestin, Ottawa, Canada). To remove unloaded PTX, the nanoparticle solution was centrifuged at 2,000 rpm for 3 min. For the measurement of loading efficiency and loading capacity, the nanoparticles were disrupted with acetonitrile and the drug content was determined by reverse-phase high-performance liquid chromatography (HPLC; Agilent Technologies, Palo Alto, CA) analysis with a 4.6×150 mm, 5-μm Sepax BR-C18 column (Sepax Technologies, Inc., Newark, Delaware) at a flow rate of 1 mL/min, using a mixture of acetonitrile and water 65:35 (*v*/*v*) as the mobile phase. A photodiode array detector was employed for detection of PTX at the wavelength of 227 nm. Under these conditions, the retention time of PTX was 3.36 min. Concentration of PTX was calculated with the help of a calibration curve constructed using solutions containing known amounts of PTX (concentration range was 1.25–80 μg/mL). Loading capacity and efficiency were calculated by following equations 1 and 2:

$$\text{Loading capacity}(\%) = \frac{\text{weight of PTX in formulation}}{\text{weight of polymer in the formulation}} \times 100 \quad (1)$$

$$\text{Loading efficiency}(\%) = \frac{\text{weight of PTX in formulation}}{\text{weight of PTX fed}} \times 100 \quad (2)$$

Hydrodynamic diameter and zeta potential were measured by dynamic light scattering (DLS) and electrophoretic light scattering (Laser Doppler) using a zeta-potential and particle size analyzer (ELSZ-1000, Otsuka Electronics Co, Osaka, Japan). Scattered light was detected at 23°C at an angle of 90°. A viscosity value of 0.933 mPa and a refractive index of 1.333 were used for data analysis.

For cryogenic-transmission electron microscopy (Cryo-TEM), CS-CE nanoparticles were applied as a drop on Lacey Formvar carbon-coated grids (Ted Pella, Redding, CA). After 30 s at RT, excess sample was removed by blotting with filter paper. The grids were then rapidly frozen in liquid ethane and observed under cryogenic conditions using a cryo-holder (626DH, Gatan) in a cryo-transmission electron microscope (CryoTecnai F20, FEI). Stability of PTX-CS-CE was determined by size measurement using DLS. To analyze time-dependent stability of PTX-CS-CE, the size of formulation was measured at 4 and 24°C for 4 weeks, while colloidal stability of formulation was analyzed by size measurement at a serial dilution (untill 400, 200, 100, 50, 20 μg/mL) to stock solution (20 mg/mL) with phosphate buffered saline (PBS; pH 7.4).

In Vitro Drug Release Study

In vitro drug release study was performed on the basis of previously reported methods with minor modifications (21, 25). PTX-CS-CE nanoparticle solution (200 μL, 2 mg/mL of PTX) was prepared and loaded in Mini-Pur-A-Lyzer tube with a molecular weight cut-off of 12 kDa (Sigma-Aldrich, Louis, MO). Tubes were immersed in 4 mL of PBS (pH 7.4) containing 0.5% (*w*/*v*) Tween 80 and incubated at 37°C. The tubes were rotated at 50 rpm. The dissolution medium (0.3 mL) was collected at various time points (1, 2, 3, 4, 6, 9, 12, 24, 48, and 72 h), and an equivalent volume of fresh medium (37°C) was added to maintain balance. The released amounts of PTX were assessed by HPLC analysis. To prepare HPLC sample, collected samples at each time point were extracted with 600 μL of ethyl-acetate twice and organic phase was then dried under high vacuum. To the dried residue was added 100 μL of acetonitrile: distill water (65:35 *v*/*v*), vortexed and followed by sonication for 10 min. Finally, 60 μL aliquot was subjected into the vial and analyzed by HPLC as described above.

In Vitro Cellular Uptake

Murine melanoma B16F10 (2×10^5 per well) and human breast adenocarcinoma MCF-7 cell lines (3×10^5 per well) were seeded in 12-well plates in Dulbecco's Modified Eagle's Medium (DMEM) supplemented with 10% fetal bovine serum followed by incubation to attach overnight. After that, the cells were exposed to PTX in Cremophor EL/Ethanol or PTX-CS-CE nanoparticle solution at a PTX concentration of 5 μg/mL for 0.5 and 2 h at 37°C. At predetermined time intervals, the cells were then washed three times with ice cold PBS to terminate the uptake and remove the PTX-loaded polymeric nanoparticles those were adsorbed on the cell membrane. Following that, cells were harvested by 0.25% Trypsin ethylenediaminetetraacetic acid (EDTA) with medium and centrifuged. To the cell pellets, 150 μL PBS (pH 7.4) was added and subjected to Bioruptor ultrasonic treatment (Bio-Medical Science, South Korea) active every 5 s for a 5 s duration with an output power of 200 W, 10 cycles in an ice bath. After sonication, 10 μL cell lysate was withdrawn and mixed with 10 μL of 0.1 μg/mL Doxetaxel (DXT) as an internal standard and extracted with ethylacetate (250 μL). The extracts were centrifuged at 14,000 rpm at 0°C for 10 min, the supernatant was dried under vacuum and after dissolving in mobile phase subjected to liquid chromatography-

mass spectrometry (LC-MS) analysis as described below. The protein content was determined using the bicinchoninic acid (BCA) protein assay kit (Thermo Fisher Scientific Inc., Rockford, IL). Cellular accumulation of PTX was normalized with reset to total protein content. Chromatography was performed using an Agilent 1100 LC (Agilent Technologies, Inc., Santa Clara, CA) with an Sepax BR-C18 1.0×100 mm, 5 μm column (Sepax Technologies, Inc., Newark, Delaware). The mobile phase consisted of phase A (0.1% formic acid in water) and phase B (100% Acetonitrile). In initial conditions, the mobile-phase composition was 10% B; a linear gradient was applied to reach a composition of 90% B after 5 min, maintained for 0.5 min and then set to return to initial conditions. The flow rate was 0.3 mL/min and volume of injected sample was 2 μL. The total HPLC effluent was directed into a 6,490 Triple Quadruple mass spectrometer (Agilent Technologies, Inc., Santa Clara, CA). Ionization was achieved using electrospray ionization in positive ion mode. The mass spectrometer was operated in multiple reaction monitoring (MRM) mode. The $(M–H)^+$ m/z transitions for PTX and DTX were 854.6→286.1 and 808.7→282.3. Typical retention times of PTX and DTX were found to be 5.84 and 5.89 min. Quantification was achieved by comparison of the observed peak area ratios of PTX and DTX in samples to a calibration curve obtained under the same conditions. The range of linear response was 0.015–10 μg/mL.

In Vitro Cytotoxicity Assay

The murine melanoma cell line B16F10 and human breast adenocarcinoma cell line MCF-7 (4×103) were grown overnight in 96-well plates in DMEM supplemented with 10% fetal bovine serum. Following this, culture medium was replaced with serum-free medium (100 μL) containing a serial dilution of each formulation up to 10 μM of PTX. After 48 h incubation, the media containing formulations were replaced with media containing 3-(4,5-dimethylthiazol-2-yl)-2,5-diphenyltetrazolium bromide (MTT, 5 mg/mL), and the plates were returned to the incubator for an additional 4 h. MTT reagent was then aspirated and DMSO was added to dissolve the formazan crystals. Color developed was quantified by measuring the absorbance at 570 nm using an Epoch microplate spectrophotometer (BioTek Instruments, Winooski, VTC). Cell viability of cells treated with PTX formulations was assessed and compared with that of control cells treated only with the medium. Cell viability was calculated via a formula reported in (26).

Pharmacokinetic Study

Animal experiment was performed according to protocols approved by the Institutional Animal Care and Use Committee at Gachon University. Pharmacokinetic study was performed in Balb-C mice (4 weeks old, 20–25 g) by dividing the animals into two groups with four animals in each. Animals were fasted for 12 h before the experiment, but had free access to water. Group I received 10 mg PTX/kg in Cremophor EL: DMSO: Water (1:5:14) per os (p.o.) and group II received PTX-CS-CE (10 mg PTX/kg) p.o. too. Blood samples (20 μL) were collected in preheparinized tube from the saphenous vein at appropriate time intervals for 8 h. At each time point, plasma (7 μL) was separated immediately by centrifuging the blood samples at 5,000 g for 5 min and stored at − 80°C until analyzed. Paclitaxel was extracted from plasma using ethylacetate and analyzed by LC-MS as described in the *in vitro* cellular uptake study to obtain the pharmacokinetic profile. Pharmacokinetic parameters were evaluated by fitting the plasma concentrations of paclitaxel using the linear trapezoid method, an add-in program for pharmacokinetic data analysis in Microsoft Excel. The relative bioavailability of PTX after oral administration was calculated using the following formula.

$$\text{Relative bioavailability} = \frac{(\text{Area Under Curve})_{PTX-CS-CE}}{(\text{Area Under Curve})_{PTX}}$$

Statistical Analysis

All of the studies were done in triplicate, and the results were expressed as mean ± standard deviation (S.D.). Statistical significance of the data was analyzed by Student's *t* test. In all of the cases $p<0.05$ was considered to be significant.

RESULTS

Characterization of CS-CE Conjugate

A scheme for the synthesis of CS-CE conjugate is shown in Fig. 2. CS-CE was synthesized by the reaction of a hydroxyl group of ceramide and the amino group of chitosan by using DSC as a coupling reagent. The significant signals at δ 0.83 and 1.21 ppm in the ^{1}H NMR spectrum of CS-CE conjugate were assigned to the resonance of methyl and alkyl chain protons, respectively, of ceramide moiety. Additionally, the signals at δ 3.04 and 4.28 ppm were attributed to the resonance of ^{2}CH-NH-COCH$_3$ and ^{1}CH-O- in chitosan moiety. Assignments of the proton signals of chitosan were made according to previous reports (27, 28). The ratio of ceramide to glucosamine in the modified chitosan was found to be 1:4 (20% of free amine groups in chitosan molecule was occupied by ceramide molecule) as assessed by ^{1}H NMR (Fig. 3a) of ceramide and chitosan moieties. Figure 3b represents the comparison of FT-IR spectra of free CS and CS-CE. The peak at 2,922.7 cm^{-1} in CS-CE conjugate corresponds to the alkyl chain of ceramide, and the peaks at 3,364.6 cm^{-1} and

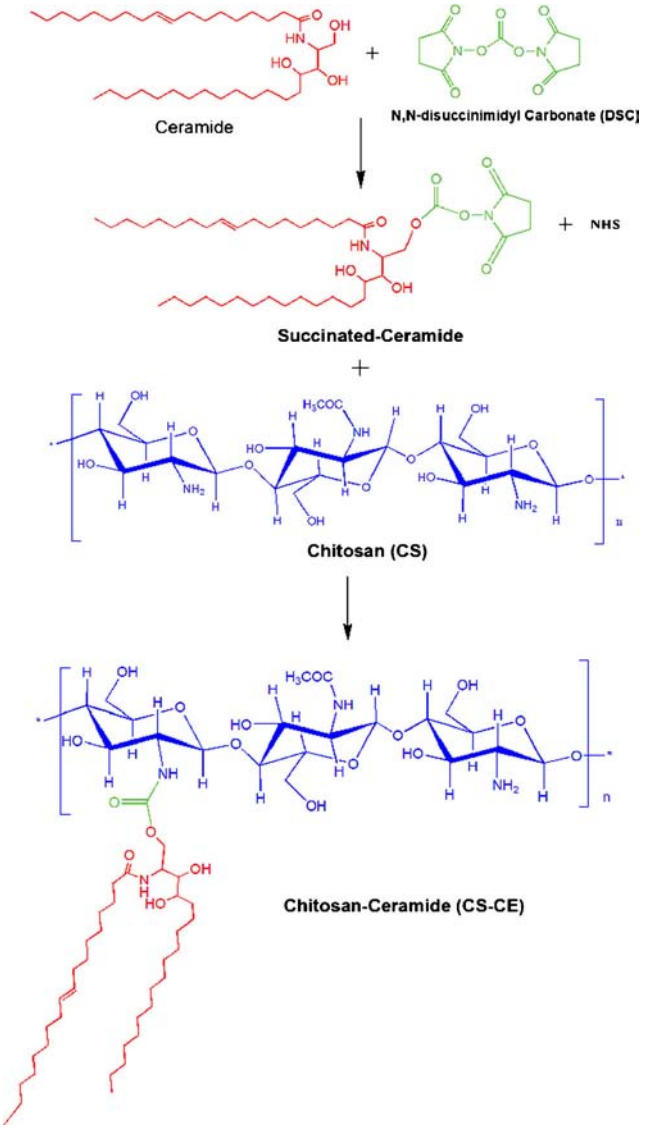

Fig. 2 Synthesis scheme of chitosan-ceramide copolymer (CS-CE).

1,015.7 cm^{-1} for the amide and the primary hydroxyl of chitosan moiety, respectively. This data confirms the formation of CS-CE conjugate.

Physicochemical Characteristics of PXT-Loaded CS-CE Nanoparticle

The scheme used for the preparation of nanoparticles is shown in Fig. 1. PTX-loaded CS-CE was prepared by emulsion-solvent evaporation method. Cryogenic transmission electron microscopy images (Fig. 4a) confirmed the formation of spherical nanoparticles. As shown in DLS profile (Fig. 4b), the particle size was bigger than that obtained by cryo-TEM, indicating that in DLS, structural analyses are carried out in solution; therefore, in that environment, the cores of the formed aggregates are swollen, and the corona is expanded (13). In addition, DLS gives more statistical 'weight' to the larger particles which are more highly scattering objects. Moreover, DLS is sensitive to the ionic environment of the nanospheres that cryo-TEM cannot visualise since it has the same density as the embedding medium (29). Due to the reasons above, the discrepancy between TEM image and DLS data could be occurred. Results of dynamic light scattering (Table 1) experiments showed that PTX-CS-CE formed nanoparticles with mean hydrodynamic diameter 305.83± 16.27 nm and zeta potential 24.16±0.59 mV, respectively. In contrast, hydrodynamic diameter and zeta potential of empty CS-CE nanoparticle were found to be 224.6 (±29.02) and 17.7 (±1.49), respectively. Loading efficiency and capacity of PTX-CS-CE were calculated to be 96.9% and 12.1%. The results of drug release study (Fig. 4c) showed that following 48-h incubation, 30% PTX is released from CS-CE nanoparticle, suggesting that the particles are efficient carrier with sustained drug release. Colloidal stability and dilution-dependent stability of PTX-CS-CE were analyzed by size measurement using DLS. The results in Fig. 5a showed that size distribution of the formulation (20 mg/mL stock) was stable up to 400-fold dilution with PBS (pH 7.4), which means this formulation could be as an intact form till around 50 μg/mL of polymer concentration. In addition, the size distribution and polydispersity index of the formulation were not changed for 28 days at 4°C and RT, respectively (Figs. 5b and c), implicating that the formulation is enough stable for storage as a solution form at least for one month.

In Vitro Quantitative Cellular Uptake

The quantitative cellular uptake of PTX-CS-CE in B16F10 and MCF-7 cells was determined to demonstrate whether the polymeric nanoparticle facilitates PTX to penetrate into the cells by LC-MS and compared with that of free PTX in Cremophor EL/ethanol at different time points. In B16F10 cells (Fig. 6a), after incubation for 2 h, the highest cellular uptake of PTX-CS-CE was observed, which was 7-fold higher than that of PTX. Following incubation for 0.5 h, PTX-CS-CE was also taken up greater than PTX by the cells. In case of MCF7 cell line (Fig. 6b), after incubation for 2 h uptake of PTX-CS-CE was significantly higher than that of PTX ($P<0.05$), while after incubation for 0.5 h uptake of PTX was slightly higher than that of PTX-CS-CE. Moreover, the uptake of PTX-CS-CE in both cells was time-dependent process which increased with time within 2 h of incubation. In contrast, in case of PTX, cellular uptake in the cells was decreased or not changed as the incubation time increased, which may be related to an aggregation of PTX in solution during the incubation or efflux pump (e.g. P-gp) which is located on the cell membrane and can efflux the drugs out cells. These results suggest that our formulation might have

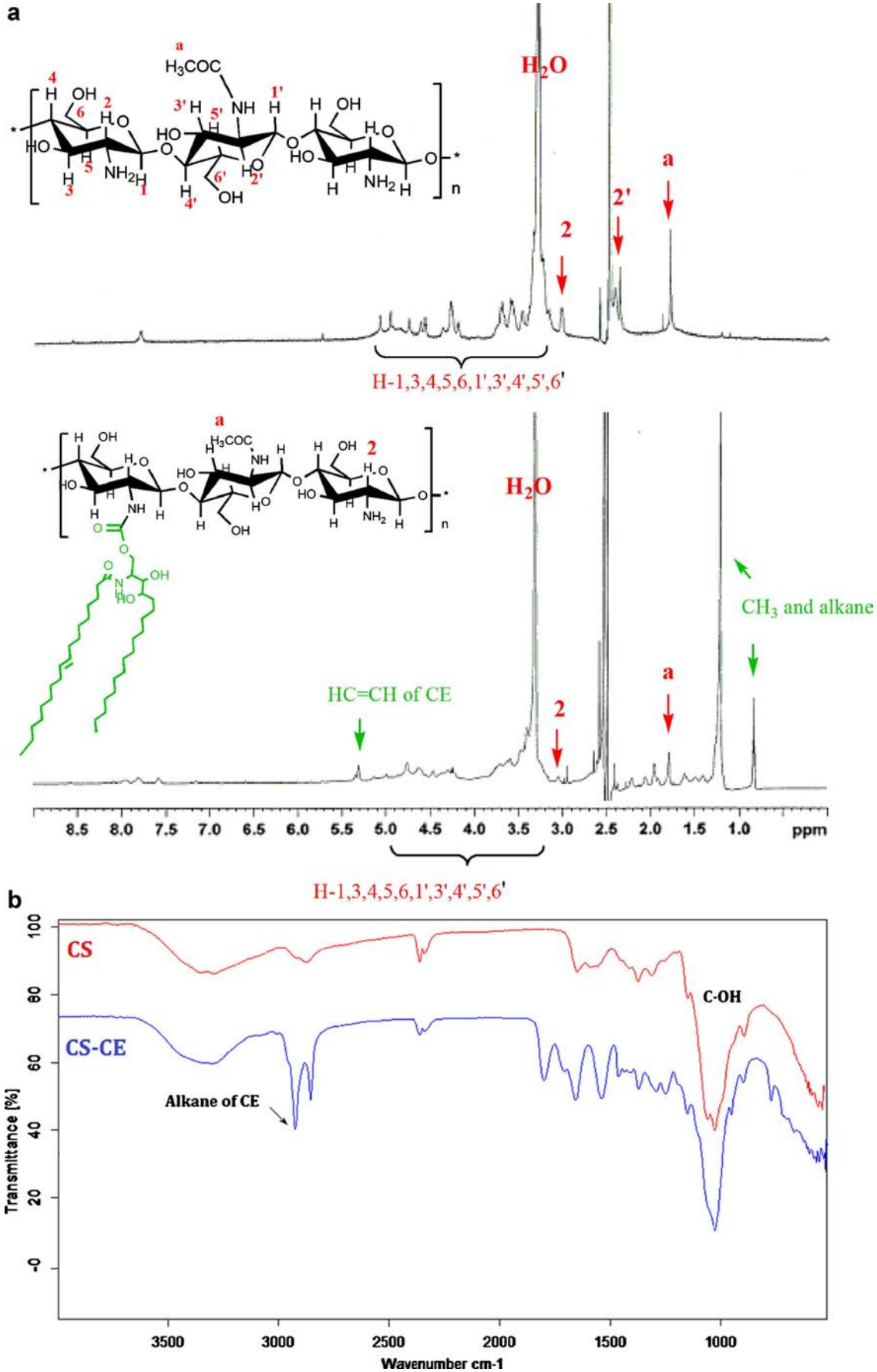
a
H2O
2'
2
a
H-1,3,4,5,6,1',3',4',5',6'
CH3 and alkane
HC=CH of CE
8.5 8.0 7.5 7.0 6.5 6.0 5.5 5.0 4.5 4.0 3.5 3.0 2.5 2.0 1.5 1.0 ppm
H-1,3,4,5,6,1',3',4',5',6'
b
CS
CS-CE
C-OH
Alkane of CE
Transmittance [%]
Wavenumber cm-1

◀ **Fig. 3** Spectra of CS-CE conjugates. 1H-NMR (**a**) and FT-IR spectra (**b**) of chitosan (CS) and chitosan-ceramide (CS-CE). In 1H NMR spectra, upper panel is for chitosan and down panel is for CS-CE.

much greater drug delivery capacity into cells due to its stability and positive surface charge.

In Vitro Cytotoxicity of PTX-Loaded CS-CE

The cytotoxic effects of CS-CE and PTX-CS-CE on B16F10 (Figs. 7a and b) and MCF-7 (Figs. 7c and d) cells over an exposure period of 72 h were evaluated by MTT assay. As shown in Figs. 7b and c, after 48 h incubation, cells treated with PTX-CS-CE showed similar viability as that of cells treated with varying concentrations of free PTX. Since PTX-loaded CS-CE nanoparticles showed higher cellular uptake as compared with free PTX, even if the formulation is capable of releasing slow, cytotoxicity effect of PTX in the formulation could be similar with that of free PTX. Empty CS-CE did not show any cytotoxicity toward the two cell lines used (Figs. 7a and c), demonstrating that the nanoparticle itself did not contribute to the cytotoxicity observed upon treatment with PTX-CS-CE nanoparticles. Although cell viability 48 and 72 h after incubation was lower than that observed 24 h post incubation, no significant difference was observed between them (data not shown).

Table 1 Physicochemical Characteristics of PTX-loaded Polymeric Nanoparticle of CS-CE (PTX-CS-CE) (mean ± S.D., $n = 3$)

Samples	LE (%)	LC (%)	Diameter (nm)	Zeta-Potential (mV)
Empty CS-CE	–	–	224.6 ± 29.02	17.7 ± 1.49
PTX-CS-CE	96.87 ± 3.2	12.1 ± 0.5	305.83 ± 16.27	24.16 ± 0.59

LE loading efficiency; *LC* loading capacity

Pharmacokinetic Study

Pharmacokinetic profile obtained after oral administration of PTX in Cremophor/DMSO/water and PTX-CS-CE nanoparticle solution at 10 mg/kg concentration of PTX in mice was shown in Fig. 8. Here, area under the curve (AUC_{0-8}) values were found to be 186.62 ± 32.2 for PTX-CS-CE and 176.81 ± 22.2 for PTX (Table 2), respectively. Maximum absorbed PTX concentration (C_{max}) in plasma was obtained 47.54 ng/mL at 0.75 h after administration for PTX-CS-CE formulation, which

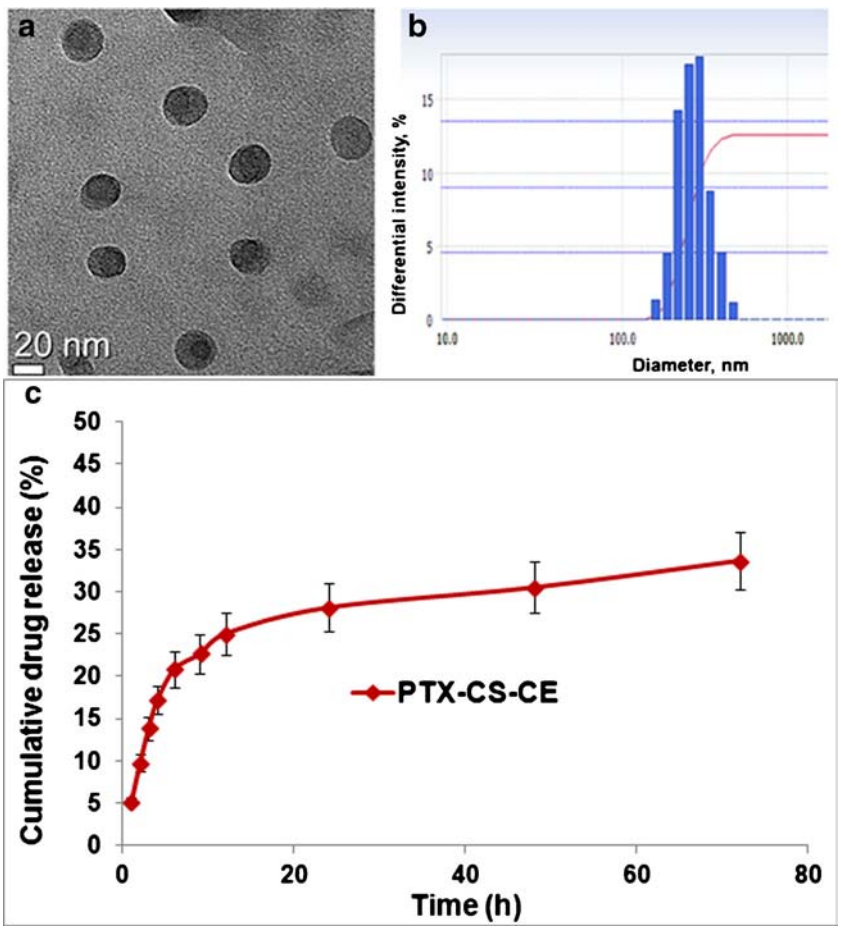

Fig. 4 Formation of paclitaxel-loaded polymeric nanoparticles of CS-CE (PTX-CS-CE): Cryo-TEM image (**a**) and size distribution (**b**) and *in vitro* release profile (**c**) of PTX from PTX-CS-CE nanoparticle (mean ± S.D., $n = 3$).

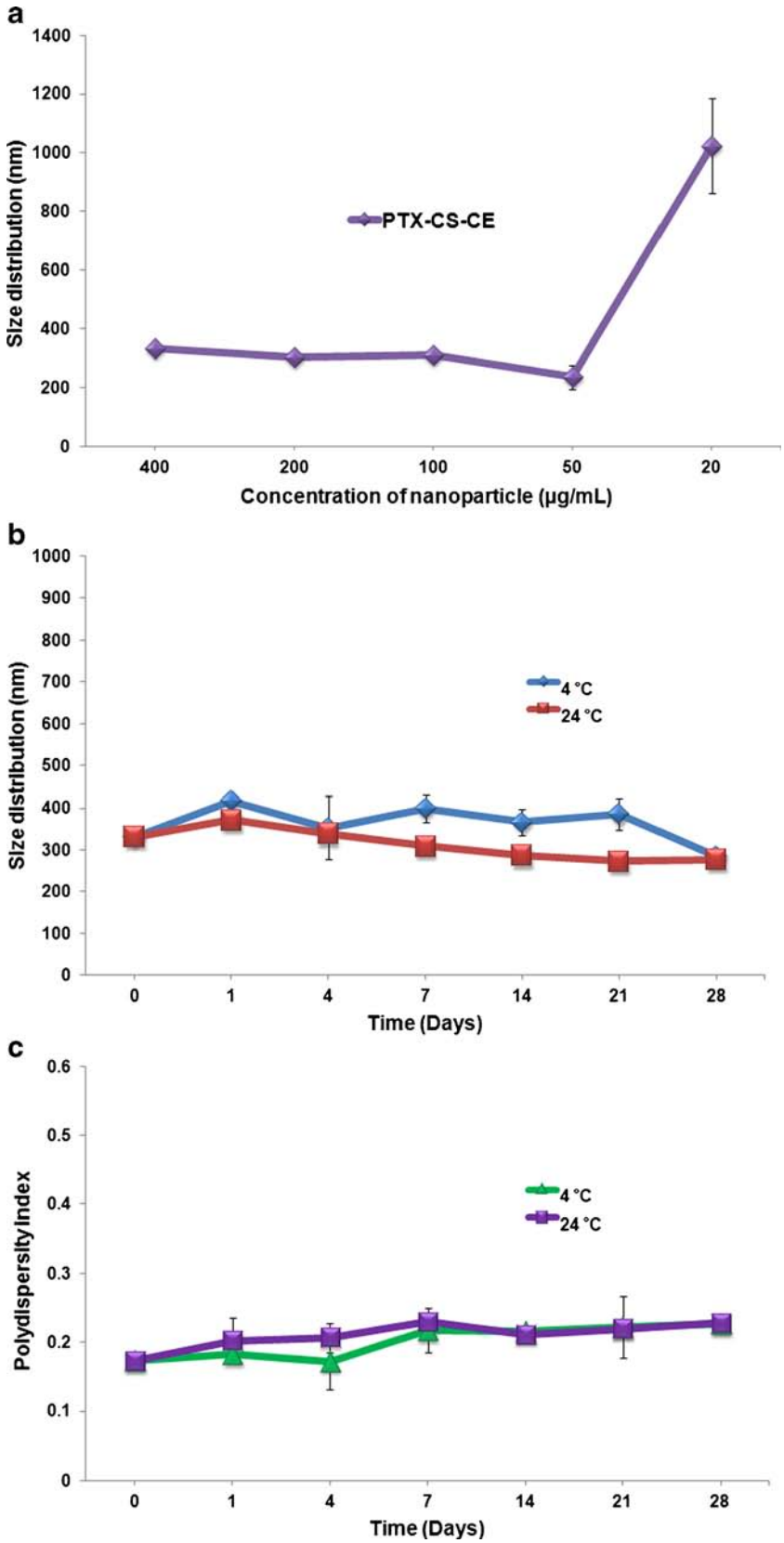

Fig. 5 Stability profiles for PTX-CS-CE nanoparticle. (**a**) Colloidal stability of PTX-CS-CE nanoparticle against dilution-induced dissociation determined by size measurement after serial dilution with PBS to 20 mg/mL and time-dependent stability of PTX-CS-CE nanoparticle as size distribution (**b**) and as polydispersity index (**c**) at 4 and 24°C for 28 days. The data represent as mean ± S.D. ($n = 3$).

was almost 2-fold higher that (28.2 ng/mL) at 0.5 h after administration of PTX in Cremophor/DMSO, indicating that the CS-CE formulation can greatly transfer a drug in the blood from the GI tract.

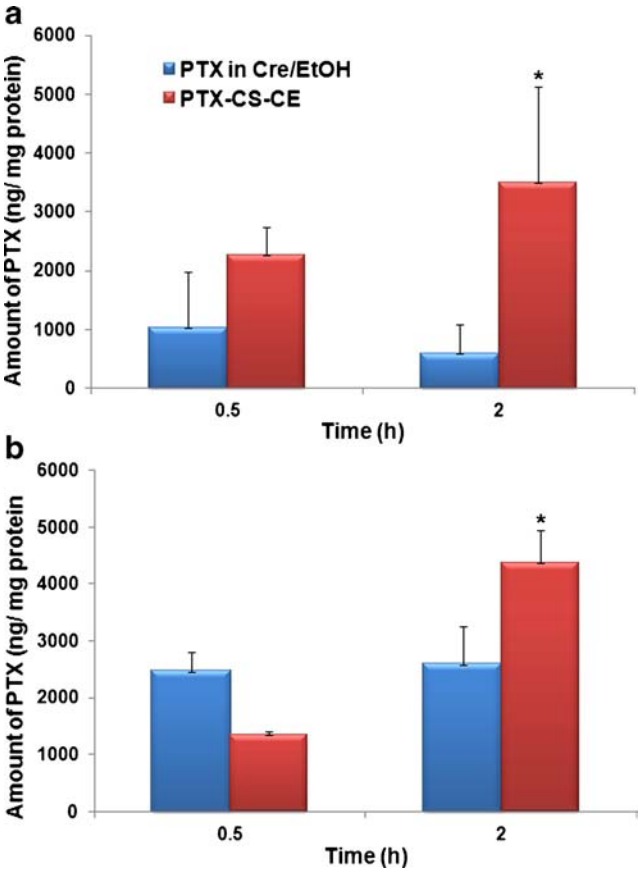

Fig. 6 Quantitative cellular uptake. Cellular levels of PTX after incubation with PTX-CS-CE and free PTX in Cremophor EL/ethanol in B16F10 (**a**) and MCF-7 (**b**) cells. *$p < 0.05$ in comparison with cells treated free PTX. The data represent as mean ± S.D. ($n = 3$).

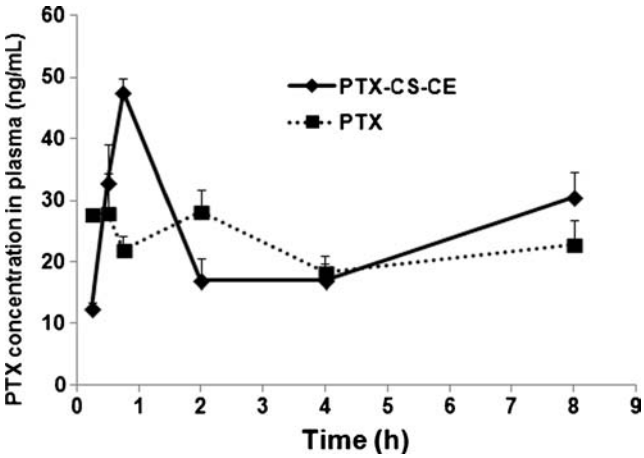

Fig. 8 Pharmacokinetic profile of paclitaxel [ng/mL] after oral administration of PTX in Cremophor EL/DMSO/H_2O and PTX-CS-CE nanoparticle solution (10.0 mg/kg). Indicated values are means (±S.E.) of three experiments. Blood samples were taken after 0.25, 0.5, 0.75, 2, 4, and 8 h.

DISCUSSION

Currently paclitaxel is administered via intravenous (i.v.) infusion by using a 1:1 (*w*/*w*) mixture of Cremophor EL and ethanol as a vehicle. Patients have to hospitalize for i.v. administration and several adverse effects have already been reported for Cremophor EL/ethanol vehicle (30). Thus, a need to develop noninvasive delivery systems for paclitaxel administration is strongly in demand. Oral administration of paclitaxel would be highly beneficial for the patients to reduce inconvenience, pain, risks of complications as well as the development of chronic treatment schedules which would decrease the cost of the therapy (5).

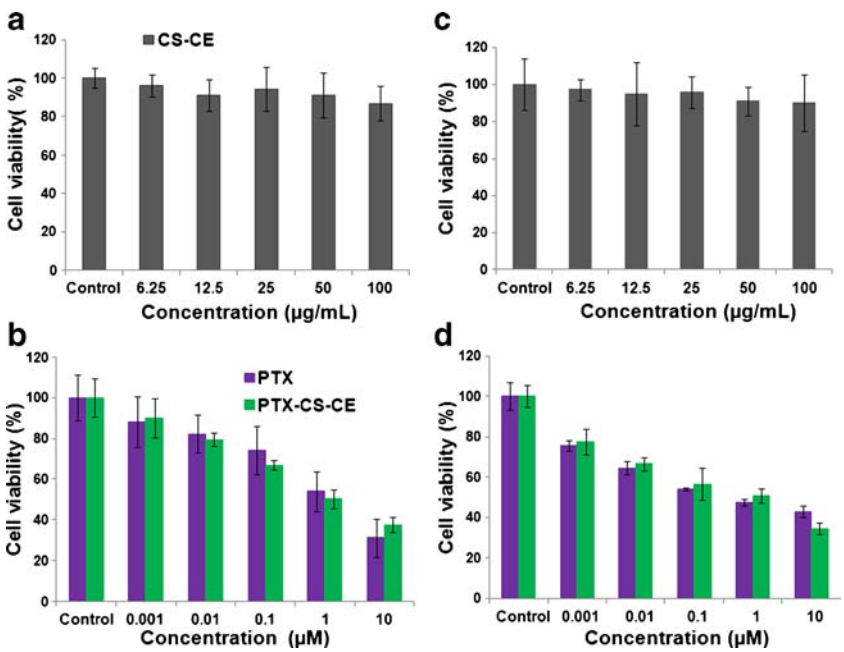

Fig. 7 *In vitro* cell viability of CS-CE and PTX-CS-CE nanoparticles in B16F10 (**a** and **b**) and MCF-7 (**c** and **d**) cells. The cell viability was analyzed after 48 h of incubation with the formulations at various concentration ranges. Concentrations of CS-CE copolymer are equivalent to those of copolymer in PTX-CS-CE nanoparticle. The data represent as mean ± S.D. ($n = 6$).

Table II Main Pharmacokinetic Parameters Calculated After Oral Administration of PTX in Cremophor EL/DMSO/Water and PTX-CS-CE Nanoparticle. Each Mouse was Given A Single Dose of 10 mg/kg PTX and Plasma Concentration-time Curves were Obtained (mean ± S.E., $n = 3$)

Parameters	PTX	PTX-CS-CE
AUC_{0-8} (h *ng/mL)	176.81 ± 22.2	186.62 ± 32.2
C_{max} (ng/mL)	28.2 ± 6.3	47.54 ± 2.3
t_{max} (h)	0.5	0.75
Relative bioavailability	–	1.055

The advantages of using nanoparticles for oral delivery of poorly adsorbed drugs include protection of drug, peptide, or nucleic acid contents from degradative enzymes, increased mucoadhesion, and increased retention in the GI tract (31, 32). It is hypothesized that this enhanced mucosal interaction is through electrostatic interactions between the positively charged nanoparticle and the negatively charged mucus and endothelial layer (33) or through a physical capture of the nanoparticle by the mucus layer (32). Nanoparticles can have greater mucoadhesive properties with the use of mucoadhesive polymers, such as chitosan (7).

Chitosan has attracted much attention as a vehicle for drug delivery owing to its biocompatibility and abundance (4, 7, 8). However, it has the limitation of being a carrier of low drug-loading capacity . Attempts made to improve the drug-loading capacity of chitosan include conjugation with fatty acids (12–16) or polyethylene glycol (34). Polysaccharides can be readily modified chemically and biochemically owing to the presence of various reactive groups (18). In this study, we synthesized chitosan-ceramide (graft copolymer) conjugate with the goal of developing a potent carrier of hydrophobic drug molecules. The structure of the conjugate was confirmed by ^{1}H NMR and FT-IR spectroscopy.

Ceramide is a component of the cell membrane and a great hydrophobic core (21) owing to its extremely hydrophobic property. In this study, we selected ceramide for chitosan modification because of the two hydrophobic chains that offer support for efficient entrapment of drugs and could form more stable core with hydrophobic drug due to its excetensive hydrophobicity (19). In previous studies, fatty acids with a single aliphatic chain have been widly used to modify chitosan backbone (12–16). The reaction between the amino group of chitosan and a hydroxyl group of ceramide in an organic solvent was successfully carried out using DSC as a coupling reagent. Although activation of hydroxyl group using DSC has been well documented (35, 36), it is rarely used for polymer conjugation. This study reveals that DSC can be used for the reactions involving hydroxyl and amino groups of a broader range of substances. We also attempted to prepare the conjugates using carbonyldiimidazole, but failed, likely because carbonyl imidazole-activated ceramide did not react with the amino group of chitosan.

We prepared PTX-loaded CS-CE nanoparticle by the emulsion-solvent evaporation method. Although we used several methods, including dialysis and evaporation for the preparation of formulations, the relatively simple emulsion-solvent evaporation method consistently provided nanoparticles with high drug loading capacity (12%). Because of PTX's bulky and rigid structure, it is often inefficiently loaded into nanomaterials (19). Consistent with previous reports, the dialysis method produced nanoparticles with a smaller size (~200 nm) and low loading efficiency (37). When the evaporation method was attempted, we found that removal of solvent was difficult due to the better solubility of our conjugates in DMSO. Our new formulation showed a sustained release of PTX. The colloidal stability result showed that our formulation was an intact form up to around 50 μg/mL concentration of polymer which was much higher than other low molar mass surfactant micelles (e.g., 1.0–24.0 mg/mL for poloxamer) (38). When the cells were treated with PTX-CS-CE, cellular uptake of PTX was getting greater as incubation time increased, indicating that the formulation could facilitate for entrapment of PTX into the cells for long time due to its stability.. Absence of cytotoxicity enables drug-loaded nanoparticles formed from CS-CE to reach the target sites such as tumors via passive targeting without harming to healthy tissues. The results of pharmacokinetic study exhibited that the formulation is a promising carrier system comparable to Cremophor EL/DMSO solution. Although some PK parameters are similar in both cases, our formulation is holding higher C_{max} and is known to be nontoxic as well; therefore, it can be used for PTX delivery. Cremophor EL/DMSO solution was selected here due to its stable suspense forming property with PTX; however, because of undesired effects of Cremophor and DMSO in patients, using as a vehicle for oral and intravenous administration of PTX always leads to obstacles. Furthermore, we were expecting that our formulation would have a much higher AUC than PTX in Cremophor/DMSO, but similar AUC was obtained, which might be a result that we used much stable formulation (5) as a control.

Our findings suggest that the novel nanoparticle developed in this study provide better alternatives to the existing toxic carriers such as cremophor EL (39).

In conclusion, we have synthesized new CS-CE conjugate that forms stable nanoparticles with improved drug loading capacity and negligible cytotoxicity. The obtained CS-CE graft-copolymer was demonstrated to be a promising carrier of hydrophobic drug, including PTX. The results of *in vivo* pharmacokinetic study promoted that our formulation could be utilized as a carrier for oral delivery of PTX.

ACKNOWLEDGMENT AND DISCLOSURES

This research was supported by the Basic Science Research Program of Korean National Research Foundation (NRF-20110007794).

REFERENCES

1. Yoo JW, Doshi N, Mitragotri S. Adaptive Micro and Nanoparticles: Temporal Control Over Carrier Properties to Facilitate Drug Delivery. Adv Drug Deliv Rev. 2011;63(14–15):1247–56.
2. Kedar U, Phutane P, Shidhaye S, Kadam V. Advances in Polymeric Micelles for Drug Delivery and Tumor Targeting. Nanomedicine. 2010;6(6):714–29.
3. Siddiqui IA, Adhami VM, Chamcheu JC, Mukhtar H. Impact of Nanotechnology in Cancer: Emphasis on Nanochemoprevention. Int J Nanomedicine. 2012;7:591–605.
4. Chen MC, Mi FL, Liao ZX, Hsiao CW, Sonaje K, Chung MF, *et al.* Recent Advances in Chitosan-based Nanoparticles for Oral Delivery of Macromolecules. Adv Drug Deliv Rev. 2013;65(6):865–79.
5. Iqbal J, Sarti F, Perera G, Bernkop-Schnurch A. Development and in vivo Evaluation of an Oral Drug Delivery System for Paclitaxel. Biomaterials. 2011;32(1):170–5.
6. Zhang L, Gu FX, Chan JM, Wang AZ, Langer RS, Farokhzad OC. Nanoparticles in Medicine: Therapeutic Applications and Developments. Clin Pharmacol Ther. 2008;83(5):761–9.
7. Gamboa JM, Leong KW. In vitro and in vivo Models for the Study of Oral Delivery of Nanoparticles. Adv Drug Deliv Rev. 2013;65(6):800–10.
8. Thanou MM, Kotze AF, Scharringhausen T, Luessen HL, de Boer AG, Verhoef JC, *et al.* Effect of Degree of Quaternization of N-Trimethyl Chitosan Chloride for Enhanced Transport of Hydrophilic Compounds Across Intestinal Caco-2 Cell Monolayers. J Control Release. 2000;64(1–3):15–25.
9. Leong KW, Sung HW. Nanoparticle-and Biomaterials-Mediated Oral Delivery for Drug, Gene, and Immunotherapy. Adv Drug Deliv Rev. 2013;65(6):757–8.
10. Hejazi R, Amiji M. Chitosan-Based Gastrointestinal Delivery Systems. J Control Release. 2003;89(2):151–65.
11. Jang MK, Jeong YI, Nah JW. Characterization and Preparation of Core-Shell Type Nanoparticle for Encapsulation of Anticancer drug. Colloids Surf B: Biointerfaces. 2010;81(2):530–6.
12. Kim K, Kwon S, Park JH, Chung H, Jeong SY, Kwon IC, *et al.* Physicochemical Characterizations of Self-Assembled Nanoparticles of Glycol Chitosan-Deoxycholic Acid Conjugates. Biomacromolecules. 2005;6(2):1154–8.
13. Liu CG, Desai KG, Chen XG, Park HJ. Linolenic Acid-Modified Chitosan for Formation of Self-Assembled Nanoparticles. J Agric Food Chem. 2005;53(2):437–41.
14. Chen XG, Lee CM, Park HJ. O/W Emulsification for the Self-Aggregation and Nanoparticle Formation of Linoleic Acid-Modified Chitosan in the Aqueous System. J Agric Food Chem. 2003;51(10):3135–9.
15. Zhang J, Chen XG, Li YY, Liu CS. Self-Assembled Nanoparticles Based on Hydrophobically Modified Chitosan as Carriers for Doxorubicin. Nanomedicine. 2007;3(4):258–65.
16. Wang XY, Zhang L, Wei XH, Wang Q. Molecular Dynamics of Paclitaxel Encapsulated by Salicylic Acid-Grafted Chitosan Oligosaccharide Aggregates. Biomaterials. 2013;34(7):1843–51.
17. Kim S, Shi Y, Kim JY, Park K, Cheng JX. Overcoming the Barriers in Micellar Drug Delivery: Loading Efficiency, in vivo Stability, and Micelle-Cell Interaction. Expert Opin Drug Deliv. 2010;7(1):49–62.
18. Liu Z, Jiao Y, Wang Y, Zhou C, Zhang Z. Polysaccharides-Based Nanoparticles as Drug Delivery Systems. Adv Drug Deliv Rev. 2008;60(15):1650–62.
19. Torchilin VP. Micellar Nanocarriers: Pharmaceutical Perspectives. Pharm Res. 2007;24(1):1–16.
20. Saddoughi SA, Song P, Ogretmen B. Roles of Bioactive Sphingolipids in Cancer Biology and Therapeutics. Subcell Biochem. 2008;49:413–40.
21. Cho HJ, Yoon HY, Koo H, Ko SH, Shim JS, Lee JH, *et al.* Self-Assembled Nanoparticles Based on Hyaluronic Acid-Ceramide (HA-CE) and Pluronic (R) for Tumor-Targeted Delivery of Docetaxel. Biomaterials. 2011;32(29):7181–90.
22. Patel MP, Patel RR, Patel JK. Chitosan Mediated Targeted Drug Delivery System: a Review. J Pharm Pharm Sci. 2010;13(4):536–57.
23. Lee E, Lee J, Lee IH, Yu M, Kim H, Chae SY, *et al.* Conjugated Chitosan as a Novel Platform for Oral Delivery of Paclitaxel. J Med Chem. 2008;51(20):6442–9.
24. Lee CM, Jang D, Kim J, Cheong SJ, Kim EM, Jeong MH, *et al.* Oleyl-Chitosan Nanoparticles Based on a Dual Probe for Optical/MR Imaging in vivo. Bioconjug Chem. 2011;22(2):186–92.
25. Zhao T, Chen H, Dong Y, Zhang J, Huang H, Zhu J, *et al.* Paclitaxel-Loaded Poly (Glycolide-Co-Epsilon-Caprolactone)-b-D-Alpha-Tocopheryl Polyethylene Glycol 2000 Succinate Nanoparticles for Lung Cancer Therapy. Int J Nanomedicine. 2013;8:1947–57.
26. Gil ES, Wu L, Xu L, Lowe TL. Beta-Cyclodextrin-Poly (Beta-Amino Ester) Nanoparticles for Sustained Drug Delivery Across the Blood–Brain Barrier. Biomacromolecules. 2012;13(11):3533–41.
27. Jiang GB, Quan D, Liao K, Wang H. Novel Polymer Micelles Prepared from Chitosan Grafted Hydrophobic Palmitoyl Groups for Drug Delivery. Mol Pharm. 2006;3(2):152–60.
28. Toh EK, Chen HY, Lo YL, Huang SJ, Wang LF. Succinated Chitosan as a Gene Carrier for Improved Chitosan Solubility and Gene Transfection. Nanomedicine. 2011;7(2):174–83.
29. Durrieu VPJ, Passas R, Gandini A. Cryo-TEM and Image Analysis of Polymer Nanoparticle Dispersions. Microsc Anal. 2004;18(1):19–21.
30. Weiss RB, Donehower RC, Wiernik PH, Ohnuma T, Gralla RJ, Trump DL, *et al.* Hypersensitivity Reactions from Taxol. J Clin Oncol. 1990;8(7):1263–8.
31. Ramesan RM, Sharma CP. Challenges and Advances in Nanoparticle-Based Oral Insulin Delivery. Expert Rev Med Devices. 2009;6(6):665–76.
32. Kawashima Y, Yamamoto H, Takeuchi H, Kuno Y. Mucoadhesive DL-Lactide/Glycolide Copolymer Nanospheres Coated with Chitosan to Improve Oral Delivery of Elcatonin. Pharm Dev Technol. 2000;5(1):77–85.
33. Ensign LM, Cone R, Hanes J. Oral Drug Delivery with Polymeric Nanoparticles: the Gastrointestinal Mucus Barriers. Adv Drug Deliv Rev. 2012;64(6):557–70.
34. Aktas Y, Yemisci M, Andrieux K, Gursoy RN, Alonso MJ, Fernandez-Megia E, *et al.* Development and Brain Delivery of Chitosan-PEG Nanoparticles Functionalized with the Monoclonal Antibody OX26. Bioconjug Chem. 2005;16(6):1503–11.
35. Miron T, Wilchek M. A Simplified Method for the Preparation of Succinimidyl Carbonate Polyethylene Glycol for Coupling to Proteins. Bioconjug Chem. 1993;4(6):568–9.
36. Morpurgo M, Bayer EA, Wilchek M. N-hydroxysuccinimide Carbonates and Carbamates are Useful Reactive Reagents for

Coupling Ligands to Lysines on Proteins. J Biochem Biophys Methods. 1999;38(1):17–28.
37. Yokoyama M, Opanasopit P, Okano T, Kawano K, Maitani Y. Polymer Design and Incorporation Methods for Polymeric Micelle Carrier System Containing Water-Insoluble Anti-Cancer Agent Camptothecin. J Drug Target. 2004;12(6):373–84.
38. Li H, Huo M, Zhou J, Dai Y, Deng Y, Shi X, *et al.* Enhanced Oral Absorption of Paclitaxel in N-deoxycholic Acid-N, O-hydroxyethyl Chitosan Micellar system. J Pharm Sci. 2010;99(11):4543–53.
39. Gelderblom H, Verweij J, Nooter K, Sparreboom A. Cremophor EL: the Drawbacks and Advantages of Vehicle Selection for Drug Formulation. Eur J Cancer. 2001;37(13):1590–8.